

# Room-temperature electroabsorption and switching in a GaAs/AlGaAs superlattice

I. Bar-Joseph, K. W. Goossen, J. M. Kuo, R. F. Kopf, D. A. B. Miller, and D. S. Chemla  
AT&T Bell Laboratories, Holmdel, New Jersey 07733

(Received 12 April 1989; accepted for publication 22 May 1989)

We report room-temperature observation of Wannier–Stark localization in a GaAs/AlGaAs superlattice. We show that large modulation can be obtained over a wide spectral range and demonstrate the operation of a self-electro-optic effect device.

Quantum well (QW) based optoelectronic devices have been rapidly evolving in the last few years. The observation of the quantum-confined Stark effect, which gives an absorption edge red shift with an applied electric field,<sup>1</sup> was followed by numerous device demonstrations. In particular, absorption and refraction light modulators were shown to operate at high speed and large contrast ratio both in the near infrared ( $\lambda \approx 0.85 \mu\text{m}$ ) and at longer wavelengths ( $\lambda \approx 1.5 \mu\text{m}$ ).<sup>2</sup> These modulators are reverse-biased  $p$ - $i$ - $n$  diodes, with the multiple quantum wells in the intrinsic region. It was also shown that the same structure can function as an optical logic switching gate, the self-electro-optic device (SEED).<sup>3</sup>

Bluse *et al.* have recently predicted that interesting behavior should occur when an electric field is applied in the growth direction of a superlattice (SL),<sup>4</sup> a structure with thin barriers between the QWs.<sup>5</sup> Because of the potential drop across the SL, the resonant tunneling process is turned off and the delocalized SL electronic wave function becomes localized. The manifestation of this phenomenon, which is called Wannier–Stark localization, is a change of the absorption edge from a broad line shape, associated with the delocalized conduction miniband, to a sharp QW-like excitonic shape, associated with the localized state. The position of the new absorption edge with field is at approximately the center of the broad miniband absorption edge without field. It corresponds, therefore, to an effective blue shift of the absorption edge. The field needed to localize the electrons is given by  $F_{\text{loc}} \approx \Delta/ed$  where  $\Delta$  is the miniband width and  $d$  is the superlattice period. At smaller fields a formation of a Stark ladder and steps in the absorption spectrum was predicted. These steps are caused by absorption from a hole state, which localizes at very low fields, to electron states in adjacent wells. They are separated by  $n(eFd)$ , where  $F$  is the electric field and  $n$  is an integer index. Correspondingly, absorption from a hole state into the nearest well is labeled as  $\pm 1$  and so forth. These steps should shift linearly with the fields away from the main absorption peak which is direct in real space.

These predictions were fully confirmed in GaAs/AlGaAs SLs using low-temperature photoconductivity,<sup>6</sup> photorefectivity,<sup>7</sup> and resonant Raman<sup>8</sup> measurements, and in InGaAs/InP SLs using transmission measurements.<sup>9</sup> In this letter we study this effect at room temperature using both photoconductivity and transmission measurements and try to determine its potential application for optoelectronic devices. We report the first room-temperature observation of Wannier–Stark localization. We show that a large

modulation can be obtained over a substantial spectral range and demonstrate the operation of a blue-shift SEED. We discuss these results in the context of present modulation techniques.

The sample is grown on an  $n^+$ -GaAs substrate followed by a  $1.3 \mu\text{m}$   $\text{Al}_{0.3}\text{Ga}_{0.7}\text{As}$   $n$ -doped  $2 \times 10^{17} \text{ cm}^{-3}$  stop etch layer. The intrinsic region is composed of a 100-period superlattice of undoped  $30 \text{ \AA}$  GaAs wells and  $30 \text{ \AA}$   $\text{Al}_{0.3}\text{Ga}_{0.7}\text{As}$  barriers. Two buffer layers of  $500 \text{ \AA}$  undoped  $\text{Al}_{0.3}\text{Ga}_{0.7}\text{As}$  separate the superlattice at both the  $n$  and the  $p$  sides. The  $p$ -doped region was composed of two  $\text{Al}_{0.3}\text{Ga}_{0.7}\text{As}$  layers, the first  $0.5 \mu\text{m}$  thick ( $p: 2 \times 10^{17} \text{ cm}^{-3}$ ) and the second  $0.3 \mu\text{m}$  ( $p^+: 2 \times 10^{18} \text{ cm}^{-3}$ ), followed by a  $1000 \text{ \AA}$  GaAs contact layer. It is important to note that the  $p$ - $i$ - $n$  junction is formed between two  $\text{Al}_{0.3}\text{Ga}_{0.7}\text{As}$  layers, setting the flatband condition at  $\approx +1.9 \text{ V}$ . The wafer was processed to form square mesas of  $200 \times 200 \mu\text{m}^2$ , which were etched to the AlGaAs stop etch layer. It was then bonded and epoxied to a sapphire substrate using transparent epoxy, and a large hole was etched through the GaAs substrate to the AlGaAs stop etch layer. A thin film of  $\text{SiO}_2$  was then deposited as an antireflection layer. The total thickness of the structure after etching the hole was approximately  $2.9 \mu\text{m}$  at the mesas and  $1.3 \mu\text{m}$  in the areas around them. Residual Fabry–Perot fringes were observed in the transmitted light, especially at the spectral regions below the gap.

The photocurrent spectra under electric field at room temperature are shown in Fig. 1. The transition from a broad to a sharp absorption edge is evident. As the voltage is increased, the Stark ladder peaks  $-1$  and  $-2$  are clearly observed and they shift linearly with the voltage away from the 0 peak. Also observed is the formation of a sharp exciton peak and its red shift with the voltage, predominantly due to a small quantum-confined Stark shift.<sup>1</sup> Comparing the results at 0 and 10 V shows a net “blue shift” of the absorption edge, with some residual absorption below the high-field edge, originating from the  $-1$  and  $-2$  peaks. This residual absorption decreases only slightly beyond 10 V.

Simulations of the absorption are in a qualitative agreement with these results. Although the heavy holes are strongly localized in one period for fields larger than  $\approx 2 \times 10^3 \text{ V/cm}$ , electrons only become strongly localized for fields larger than  $\approx 8 \times 10^4 \text{ V/cm}$ , which is approximately the field at which the central peak becomes dominant in the spectra. The simulations also show, however, that the electron wave function is not fully localized in one period even at these fields, confirming the experimental observation that there is still residual absorption at high voltages for the

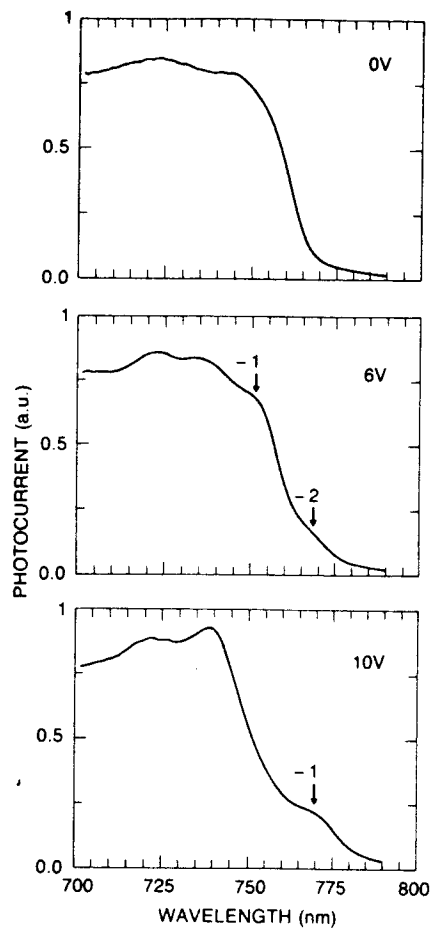


FIG. 1. Room-temperature photocurrent spectra for 0, 6, and 10 V.

— 1 and — 2 peaks.

At high fields, when both electrons and holes are localized, the optical transitions show clear excitonic enhancement, reminiscent of that seen for quasi-two-dimensional (2D) excitons in QW structures. Let us note, however, that this analogy applies well only to the direct transition. For the other transitions,  $\pm 1$ ,  $\pm 2$  electrons and holes are localized in thin layers which are spatially separated. Since the SL period is smaller than the bulk Bohr radius ( $a_0 = 140 \text{ \AA}$ ), electrons and holes in adjacent wells are still correlated. This correlation reduces with the separation and so does the wave function overlap. The excitonic enhancement is, therefore, expected to follow the transition strength. This is indeed what we observe experimentally.

At low fields the excitonic features significantly decrease, and there is hardly any evidence of their presence at 0 V. Let us note, however, that the built-in field across the  $p-i-n$  junction at that voltage is  $2.7 \times 10^4 \text{ V/cm}$ . At such a field the holes are localized while the electrons are delocalized. Because the electrons are free to move in the direction of the field, it is expected that unlike in 2D the excitons would be field ionized at low fields. A detailed study of the excitonic behavior especially close to the flatband condition is left for a different publication.

To determine the actual absorption changes with field, we measured the differential transmission spectra. This was

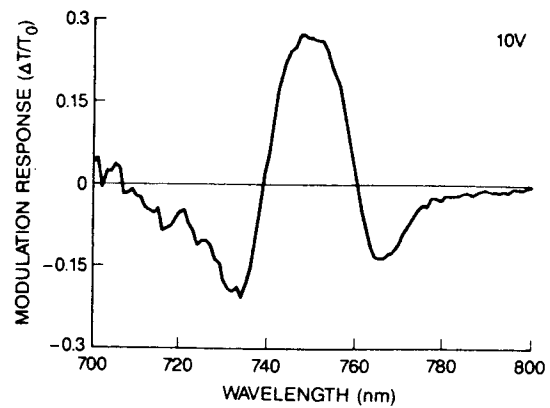


FIG. 2. Modulation response ( $\Delta T/T_0$ ) as a function of wavelength for a square wave modulation between 0 and  $-10 \text{ V}$  ( $T_0$  is taken as the transmission at  $0 \text{ V}$ ).

done by applying a square wave voltage modulation between  $0 \text{ V}$  and a certain reverse bias  $V$ , and detecting the corresponding transmission changes with a lock-in. Figure 2 shows such a spectrum for  $V = -10 \text{ V}$ , where a positive signal corresponds to an induced transmission and a negative one to induced absorption. The origin of the main positive peak at  $750 \text{ nm}$  is the effective "blue shift" of the absorption edge. The negative peak at  $730 \text{ nm}$  is due to the QW exciton which is formed at high fields, and the one at  $770 \text{ nm}$  is due to the residual absorption from the  $-1$  Stark ladder transition which is shifted to that wavelength.

Because of the complex changes of the absorption spectrum with field, which involve formation of a few peaks which are shifting in energy and changing in strength, the differential transmission spectra for other voltages can be very different from the one for  $-10 \text{ V}$ . This is reflected in the nonlinear behavior of the modulation response ( $\Delta T/T_0$ , where  $T_0$  is the transmission at  $0 \text{ V}$ ) with field, as depicted in Fig. 3 for  $\lambda = 750 \text{ nm}$ . At lower voltages we get a slow increase, which then becomes very sharp around  $V = 5 \text{ V}$ . At higher voltages ( $V > 10 \text{ V}$ ) there is a saturation, and there is not much gain of modulation depth beyond  $15 \text{ V}$ . The value of  $\Delta T/T_0$  for  $15 \text{ V}$ , which is  $0.37$ , corresponds to  $\Delta\alpha = 7700 \text{ cm}^{-1}$  which is a remarkable electroabsorption value. It can,

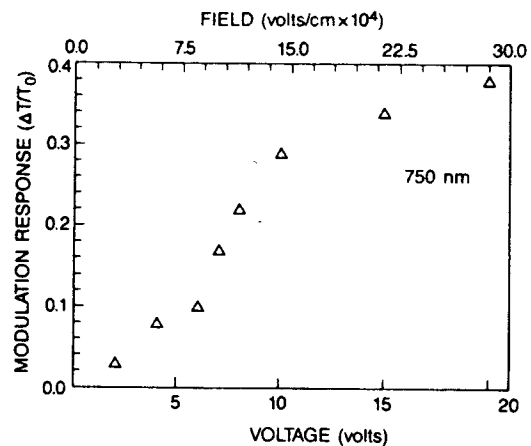


FIG. 3. Modulation response ( $\Delta T/T_0$ ) as a function of voltage for a square wave modulation between  $0 \text{ V}$  and that voltage ( $T_0$  is taken as the transmission at  $0 \text{ V}$ ).

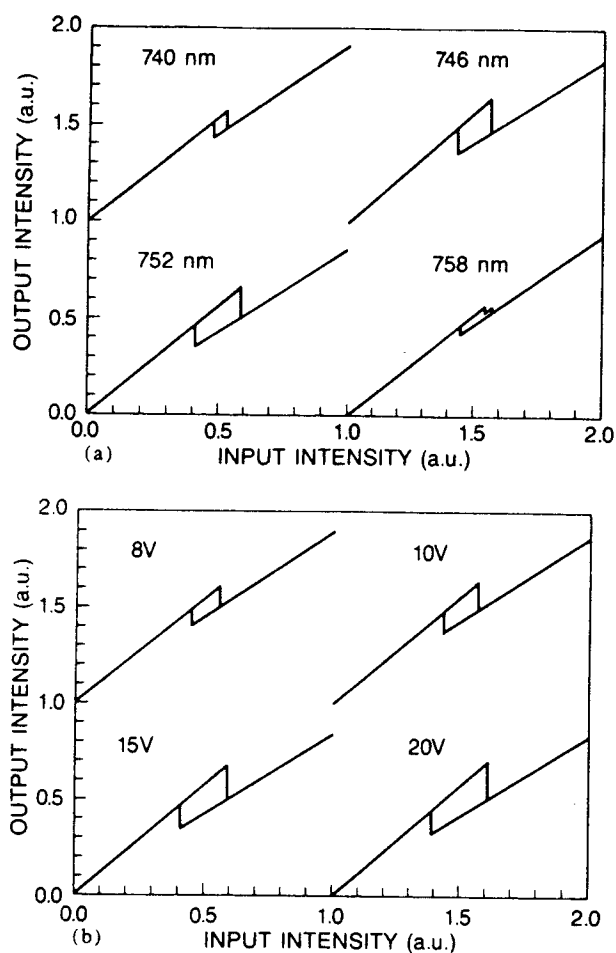


FIG. 4. Output intensity as a function of input intensity for (a) several wavelengths and (b) several voltages.

connected the SL diode in series to a silicon photodiode, which when illuminated with white light acted as a current source load. We used a tungsten lamp and a 0.22 m SPEX spectrometer as a monochromatic illumination source for the SL diode. Figures 4(a) and 4(b) show the bistable behavior for different wavelengths and voltages, respectively. It can be seen that bistability is obtained over a wide spectral range and is almost constant between 745 and 755 nm. The voltage dependence is in agreement with the modulation response values of Fig. 3. This agreement is to be expected since the voltage on the SL diode switches approximately between the bias voltage and 0 V. Clear bistability is observed at 8 V, and there is not much change beyond 15 V.

This observation of room-temperature electroabsorption in SL structures and the demonstration of high contrast modulation and switching behavior may set the stage for a new class of optoelectronic devices. One potential advantage of these structures compared to QW modulators is that it may be easier to sweep carriers out of the structure because of the lower effective barriers for tunneling and thermionic emission. This may reduce problems resulting from saturation and space-charge buildup due to holes accumulation, that can prevent high-power operation of modulators and high-speed operation of SEEDs. The superlattice electroabsorption may also give a larger usable spectral bandwidth because it relies less on sharp exciton resonances.

therefore, be projected that a  $1\text{ }\mu\text{m}$  SL structure would yield a 2:1 modulation ratio for  $V = -20\text{ V}$ . The sharp rise at medium voltages can be exploited to generate a large response at low modulation swing. When the structure is biased at  $-5\text{ V}$ , we can obtain a modulation of  $1500\text{ cm}^{-1}/\text{V}$ .

The responsivity curves for this structure, which describe the photocurrent as a function of voltage for a given wavelength, exhibit a rich behavior with regions of negative differential resistance. This is especially the case at the spectral regions near the SL absorption edge; the decreased absorption with the blue shift of the absorption edge yields a decrease in the photocurrent and, therefore, a negative differential resistance. This behavior can be used to construct a logic element, similar to the self-electro-optic device (SEED), which is based on a blue shift<sup>10</sup> rather than the red shift associated with the quantum-confined Stark effect. We

<sup>1</sup>D. A. B. Miller, D. S. Chemla, T. C. Damen, A. C. Gossard, W. Wiegmann, T. H. Wood, and C. A. Burrus, *Phys. Rev. B* **32**, 1043 (1985).

<sup>2</sup>T. H. Wood, C. A. Burrus, D. A. B. Miller, D. S. Chemla, T. C. Damen, A. C. Gossard, and W. Wiegmann, *IEEE J. Quantum Electron.* **QE-21**, 117 (1985); U. Koren, B. I. Miller, T. L. Koch, G. Eisenstein, R. S. Tucker, I. Bar-Joseph, and D. S. Chemla, *Appl. Phys. Lett.* **51**, 1132 (1987).

<sup>3</sup>D. A. B. Miller, D. S. Chemla, T. C. Damen, T. H. Wood, C. A. Burrus, A. C. Gossard, and W. Wiegmann, *IEEE J. Quantum Electron.* **QE-21**, 1462 (1985).

<sup>4</sup>J. Bleuse, G. Bastard, and P. Voisin, *Phys. Rev. Lett.* **60**, 220 (1988).

<sup>5</sup>L. Esaki and R. Tsu, *IBM J. Res. Dev.* **14**, 61 (1970).

<sup>6</sup>E. E. Mendez, F. Agullo-Rueda, and J. M. Hong, *Phys. Rev. Lett.* **60**, 2426 (1988).

<sup>7</sup>P. Voisin, J. Bleuse, C. Bouche, S. Gaillard, and C. Alibert, *Phys. Rev. Lett.* **61**, 1639 (1988).

<sup>8</sup>F. Agullo-Rueda, E. E. Mendez, and J. M. Hong, *Phys. Rev. B (Rapid Commun.)* **38**, 12 720 (1988).

<sup>9</sup>J. Bleuse, P. Voisin, M. Allovon, and M. Quillec, *Appl. Phys. Lett.* **53**, 2632 (1988).

<sup>10</sup>D. A. B. Miller, *Appl. Phys. Lett.* **54**, 202 (1989).